Original Article

Arterial spin labeling combined with T1 mapping for assessment of kidney function and histopathology in patients with long-term renal transplant survival after kidney transplantation

Bin Jiang[1#], Jie Li[2#], Jiayi Wan[1], Yangyang Tian[3], Peng Wu[4], Rui Xu[1], Yixing Yu[1], Ximing Wang[1], Linkun Hu[3], Mo Zhu[1]

[1]Department of Radiology, The First Affiliated Hospital of Soochow University, Suzhou, China; [2]Suzhou Medical College, Soochow University, Suzhou, China; [3]Department of Urology, The First Affiliated Hospital of Soochow University, Suzhou, China; [4]Philips Healthcare, Shanghai, China

Contributions: (I) Conception and design: L Hu, M Zhu; (II) Administrative support: L Hu, M Zhu, Y Yu, X Wang; (III) Provision of study materials or patients: Y Tian, L Hu; (IV) Collection and assembly of data: B Jiang, J Li, J Wan, R Xu; (V) Data analysis and interpretation: B Jiang, P Wu; (VI) Manuscript writing: All authors; (VII) Final approval of manuscript: All authors.

[#]These authors contributed equally to this work.

Correspondence to: Linkun Hu, MD. Department of Urology, The First Affiliated Hospital of Soochow University, No. 899 Pinghai Road, Suzhou 215006, China. Email: hulinkunsz@163.com; Mo Zhu, MD. Department of Radiology, The First Affiliated Hospital of Soochow University, No. 899 Pinghai Road, Suzhou 215006, China. Email: soochowzhumo@163.com.

Background: The long-term survival of kidney transplants is often influenced by various factors, among which renal allograft rejection is the most notable factor. A noninvasive and reliable imaging biomarker correlating with kidney function and histopathology would facilitate longitudinal long-term follow-up of renal allografts. The aim of the study is to investigate the value of arterial spin labeling (ASL) combined with T1 mapping for assessing kidney function in patients with long-term renal transplant survival, and to establish radiological and histopathologic correlations between the magnetic resonance imaging (MRI) measurements and kidney allograft biopsy findings.

Methods: Kidney transplant recipients who were admitted to the Department of Urology in First Affiliated Hospital of Soochow University between January and December 2022 were prospectively consecutively recruited [group A, estimated glomerular filtration rate (eGFR) ≥60 mL/min/1.73 m^2; group B, 30≤ eGFR <60 mL/min/1.73 m^2; group C, eGFR <30 mL/min/1.73 m^2], and part of them underwent biopsies. All patients underwent ASL and T1 mapping. MRI parameters were calculated and analyzed.

Results: A total of 63 patients (Group A, 30 cases; Group B, 20 cases; and Group C, 13 cases) were included in this cross-sectional study. Cortical T1 increased, whereas renal blood flow (RBF) and ΔT1 [100% × (cortical T1 – medullary T1)/cortical T1] decreased with the decrease of eGFR. The RBF, cortical T1, and ΔT1 values were moderately correlated with eGFR (r=0.569, –0.573, and 0.672, respectively). The MRI parameters were moderately correlated with Banff scores, which determined renal allograft rejection and chronicity. The area under the curve (AUC) for the discrimination of groups A versus B and groups A versus C were 0.740 [95% confidence interval (CI): 0.597–0.854, P=0.004] and 0.923 (95% CI: 0.800–0.982, P<0.001), respectively, using ASL; 0.873 (95% CI: 0.749–0.950, P<0.001) and 0.926 (95% CI: 0.803–0.983, P<0.001), respectively, using T1 mapping; and 0.892 (95% CI: 0.771–0.962, P<0.001) and 0.956 (95% CI: 0.846–0.995, P<0.001), respectively, using multi-parameter MRI. The AUC for discrimination between groups B and C was 0.729 (95% CI: 0.546–0.868, P=0.02) using ASL.

Conclusions: The RBF, cortical T1, and ΔT1 can serve as new imaging biomarkers of kidney function and histopathological microstructure.

Keywords: Acute rejection; arterial spin labeling (ASL); magnetic resonance imaging (MRI); mapping; renal transplantation

Submitted Nov 07, 2023. Accepted for publication Jan 10, 2024. Published online Mar 04, 2024.
doi: 10.21037/qims-23-1577
View this article at: https://dx.doi.org/10.21037/qims-23-1577

Introduction

In patients with kidney failure, renal transplantation is the optimal treatment option compared to dialysis. However, the main primary independent risk factor for the long-term survival of a transplanted kidney is renal allograft rejection (1). With the widespread implementation of tissue-matching techniques, perioperative antibody induction therapy, and the utilization of new immunosuppressive agents, the incidence of acute rejection is decreasing every year (2). Owing to the limited number of kidney donors and the increasing number of patients requiring kidney transplants, it is essential to maintain the function of a transplanted kidney for as long as possible (3). Creatinine is the most widely used laboratory index for clinical monitoring of kidney function. However, it may not be adequately sensitive to detect rapid changes in kidney function till more than half of the kidney function is lost (4,5). This time lag may lead to delayed treatment, resulting in a poor prognosis of the transplanted kidney (6). An ultrasound can noninvasively monitor postoperative vascular and surgical complications in transplanted kidneys. The ultrasound examination strongly relies on the operator's experience and has low sensitivity. A biopsy remains the gold standard for diagnosing diseases of transplanted kidneys. Although generally safe, sedation and anesthesia carry the risks of procedural bradycardia, hypoxemia, and aspiration, which cannot be neglected (7-11).

Magnetic resonance imaging (MRI) can provide morphological, functional, and microstructural information about the transplanted kidney (12-14). In addition, MRI is operator-independent and can be obtained without contrast agents and radiation exposure; thus allowing multiple examinations to be performed. Arterial spin labeling (ASL) can be used to label inflowing blood as an endogenous contrast agent. It is proven that renal blood perfusion measured using ASL is comparable to that measured using fluorescent microspheres and dynamic contrast enhancement (15,16); hence, tissue microvascular perfusion can be repeatedly and accurately evaluated. T1 mapping allows the direct measurement of T1 relaxation time (17), which quantifies small changes in tissues (18). It helps to noninvasively evaluate the parenchymal changes in a transplanted kidney. T1 mapping has been widely used in the heart (19,20) and other organs to assess tissue edema and fibrosis. However, its use in transplanted kidneys is relatively rare.

In this study, we investigated the structural and functional changes with respect to renal tissue microstructure and perfusion in patients with long-term renal transplant survival. We aimed to explore the potential of multi-parametric MRI (mpMRI), including ASL and T1 mapping, to assess kidney function and act as a noninvasive imaging biomarker of histopathological changes in transplanted kidneys. We present this article in accordance with the STROBE reporting checklist (available at https://qims.amegroups.com/article/view/10.21037/qims-23-1577/rc).

Methods

Study population

We prospectively consecutively recruited kidney transplant recipients who were admitted to the Department of Urology in the First Affiliated Hospital of Soochow University between January and December 2022 for the cross-sectional study. The study was conducted in accordance with the Declaration of Helsinki (as revised in 2013). The study was approved by ethics board of the First Affiliated Hospital of Soochow University and informed consent was obtained from all the patients. All participants underwent ASL and T1 mapping. Adult patients who had undergone kidney transplant surgery >3 months were included. The exclusion criteria were as follows: (I) contraindications to magnetic resonance (MR) examination; (II) complications including transplanted kidney infarction, bleeding, and transplanted renal artery stenosis; (III) fail to complete all MRI examination; (IV) poor image quality (*Figure 1*). The patients' serum creatinine levels were recorded on the day of the MRI. The estimated glomerular filtration rate (eGFR) was calculated using the Chronic Kidney Disease Epidemiology Collaboration (CKD-EPI)

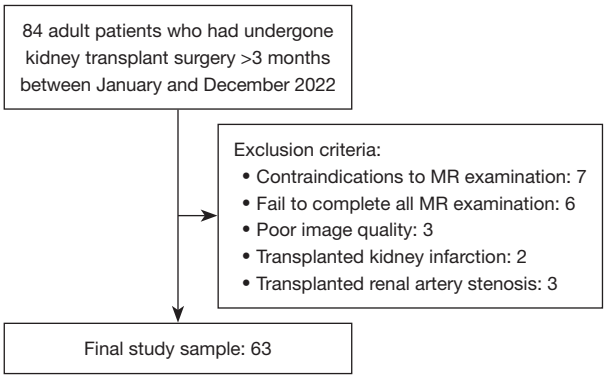

Figure 1 Flowchart of study inclusion and exclusion criteria. MR, magnetic resonance.

formula (21). Based on the eGFR, the patients were divided into three groups: Group A, patients with normal to mildly reduced eGFR (eGFR ≥60 mL/min/1.73 m^2); Group B, patients with moderately reduced eGFR (30≤ eGFR <60 mL/min/1.73 m^2); and Group C, patients with severely reduced eGFR (eGFR <30 mL/min/1.73 m^2).

MRI protocols

All patients were scanned using a 1.5 T MRI scanner (Ingenia Ambition, Philips Healthcare, Best, Netherlands) equipped with a 28-channel phased-array coil. The scan range extended from the inferior border of the rib arch to the inferior border of the pubic symphysis. Coronal T2-weighted and axial T1-weighted images (T1WI) were acquired for morphological evaluation. For the pseudo-continuous ASL (pCASL) sequence, three-dimensional (3D) gradient and spin-echo (GRASE) acquisition were used. Image parameters for pCASL were as follows: repetition time (TR), 3,963 ms; echo time (TE), 15 ms; voxel size, 3.75×3.75×8 mm^3; field of view (FOV), 240×240×88 mm^3; turbo spin echo (TSE) factor, 20; echo planar imaging (EPI) factor, 15; and eight dynamics. The scan parameters for T1 mapping were as follows: a modified Look-Locker inversion-recovery (MOLLI) acquisition scheme, TR, 2.8 ms; TE, 1.3 ms; flip angle, 35°; voxel size, 2.2×2.2 mm^2; FOV, 300×300 mm^2; slice thickness, 5 mm; and five slices.

Image analysis

All raw images were loaded onto a workstation (IntelliSpace Portal v10; Philips Healthcare). For ASL, the renal cortical contour was manually outlined on the axial T1WI and simultaneously copied to the renal blood flow (RBF) map. For T1 mapping, the renal cortical contour was manually outlined on the coronal T2-weighted images (T2WI), and several elliptical regions of interest (ROI) were placed on the medulla and copied to the T1 map. The ΔT1 was defined as [100% × (cortical T1 – medullary T1)/cortical T1], which could reflect the difference in T1 values between the renal cortex and medulla. The size of the medullary ROI was 5–25 mm^2. The ROIs were selected by avoiding areas with blood vessels, hematomas, and cysts. Two abdominal radiologists, with 8 and 10 years of experience, independently and randomly analyzed all images without referring to clinical or pathologic data.

Renal allograft biopsy

Twenty patients underwent an ultrasonography-guided percutaneous renal transplant biopsy. The interval between biopsy and MRI examination was <48 h. The kidney transplant biopsies were evaluated based on the Banff classification, a standardized system of grading and nomenclature for renal allograft pathology (22). In the Banff classification, the severity of specific histologic findings is represented by quantitative pathologic scores, which serve as a morphologic foundation for the diagnosis of cellular and antibody-mediated rejections (23). In our study, the Banff scores related to tubular, vascular, and glomerular rejection were collected and analyzed. The major Banff pathological scores included tubular atrophy (ct score), interstitial fibrosis (ci score), peritubular capillaritis (ptc score), glomerulonephritis (g score), interstitial inflammation (i score), and tubulitis (t score). Tubulitis and interstitial inflammation are important pathological changes in acute T cell-mediated rejection (aTCMR), and peritubular capillaritis and glomerulonephritis are characteristic pathological changes in active antibody-mediated rejection (aAMR) (24). Tubular atrophy and interstitial fibrosis indicate chronicity (22).

Statistical analysis

Statistical analysis was performed using the SPSS 25 statistical software. Data normality was tested using the Kolmogorov-Smirnov test. In the case of measurement data conforming to a normal distribution, it was represented as mean ± standard deviation. Between-group comparisons were conducted using one-way analysis of variance (ANOVA), followed by pairwise comparisons

Table 1 Overview of study characteristics

Characteristics	Group A	Group B	Group C	Total	P
Nnt (male/female)	30 (15/15)	20 (16/4)	13 (9/4)	63 (40/23)	0.17
Age (years), mean ± SD	42.4±8.0	41.6±9.1	48.4±10.2	43.4±9.1	0.08
eGFR (mL/min/1.73 m^2), mean ± SD	82.2±17.5	46.1±8.3*	23.6±3.7*#	58.7±27.2	<0.001
SCr (μmol/L), mean ± SD	89.9±24.0	155.5±28.9*	254.9±58.5*#	144.8±72.3	<0.001
Hemoglobin (g/L), mean ± SD	137.6±19.2	121.5±15.5*	105.9±15.9*#	126.0±21.2	<0.001
CysC (mg/L), mean ± SD	1.24±0.24	1.96±0.51*	2.82±0.66*#	1.79±0.75	<0.001
Length (mm), mean ± SD	113.6±13.0	111.6±12.9	103.2±15.3	110.8±13.9	0.07
Transplanted time (months), M [Q1, Q3]	12 [8–36]	44 [25–62]*	72 [14–154]*	28 [11–60]	0.001
RBF (mL/100 g/min), mean ± SD	221.2±52.1	172.0±63.8*	122.6±46.5*#	185.2±66.6	<0.001
Cortical T1 (ms), mean ± SD	1,284.5±114.6	1,384.3±103.7*	1,456.3±106.3*	1,351.6±128.3	<0.001
Medullary T1 (ms), mean ± SD	1,784.1±102.8	1,723.4±120.0	1,800.3±112.5	1,768.2±113.0	0.09
ΔT1 (%), mean ± SD	39.5±10.0	24.9±9.2*	23.9±6.0*	31.7±11.7	<0.001

Group A, patients with normal to mildly reduced eGFR (eGFR ≥60 mL/min/1.73 m^2); Group B, patients with moderately reduced eGFR (30≤ eGFR <60 mL/min/1.73 m^2); and Group C, patients with severely reduced eGFR (eGFR <30 mL/min/1.73 m^2). *, compared with Group A (*P<0.05); #, compared with Group B (#P<0.05). P denotes comparisons among the three groups. SD, standard deviation; eGFR, estimated glomerular filtration rate; SCr, serum creatinine; CysC, Cystatin C; RBF, renal blood flow; T1, longitudinal relaxation time; ΔT1, 100% × (cortical T1 – medullary T1)/cortical T1.

using the Bonferroni method. Non-normally distributed measurement data were represented as M (Q1, Q3), and between-group comparisons were conducted using the Kruskal-Wallis H test. Categorical variable comparisons were conducted using the Chi-squared test or Fisher's exact probability method. The repeatability of MRI measurements among observers was assessed using the intraclass correlation coefficient (ICC). An independent sample *t*-test was used to test the corticomedullary differences of T1. The correlation between MRI parameters and eGFR was analyzed using Pearson's correlation coefficient. The Spearman rank correlation coefficients were calculated to investigate the relationship between MRI parameters and Banff pathological scores. The performance of MRI parameters in detecting the degree of allograft impairment was assessed using the receiver operating characteristic (ROC) curve. Post-hoc pairwise comparisons were conducted using the DeLong test. A two-sided P value<0.05 was set to represent statistical significance.

Results

Patient characteristics

Sixty-three patients were included in this study. A brief overview of the study characteristics is provided in *Table 1*. Detailed information on biopsy results is presented in Table S1.

Inter-observer reproducibility for MRI measurements

All the MRI parameters showed excellent agreement. The ICCs were 0.920, 0.943, and 0.920 for cortical RBF, cortical T1, and medullary T1, respectively.

Differences in MRI parameters between the groups

RBF tended to decrease with the decrease of eGFR, and this difference was statistically significant (P<0.001). It was higher in group A (221.2±52.1 mL/100 g/min) than that in groups B (172.0±63.8 mL/100 g/min, P=0.009) and C (122.6±46.5 mL/100 g/min, P<0.001). Additionally, RBF was higher in group B than that in group C (P=0.04). Cortical T1 was shorter in group A (1,284.5±114.6 ms) than that in groups B (1,384.3±103.7 ms, P=0.008) and C (1,456.3±106.3 ms, P<0.001). The ΔT1 was larger in group A (39.5%±10.0%) than that in groups B (24.9%±9.2%, P<0.001) and C (23.9%±6.0%, P<0.001). No significant difference was observed in the medullary T1 among the three groups (P=0.09). In all three groups, medullary T1 was significantly longer than cortical T1 (P<0.001) (*Table 1*, *Figure 2*).

Relationships between MRI parameters, eGFR, and Banff histopathology scores

The RBF and ΔT1 were positively correlated with eGFR

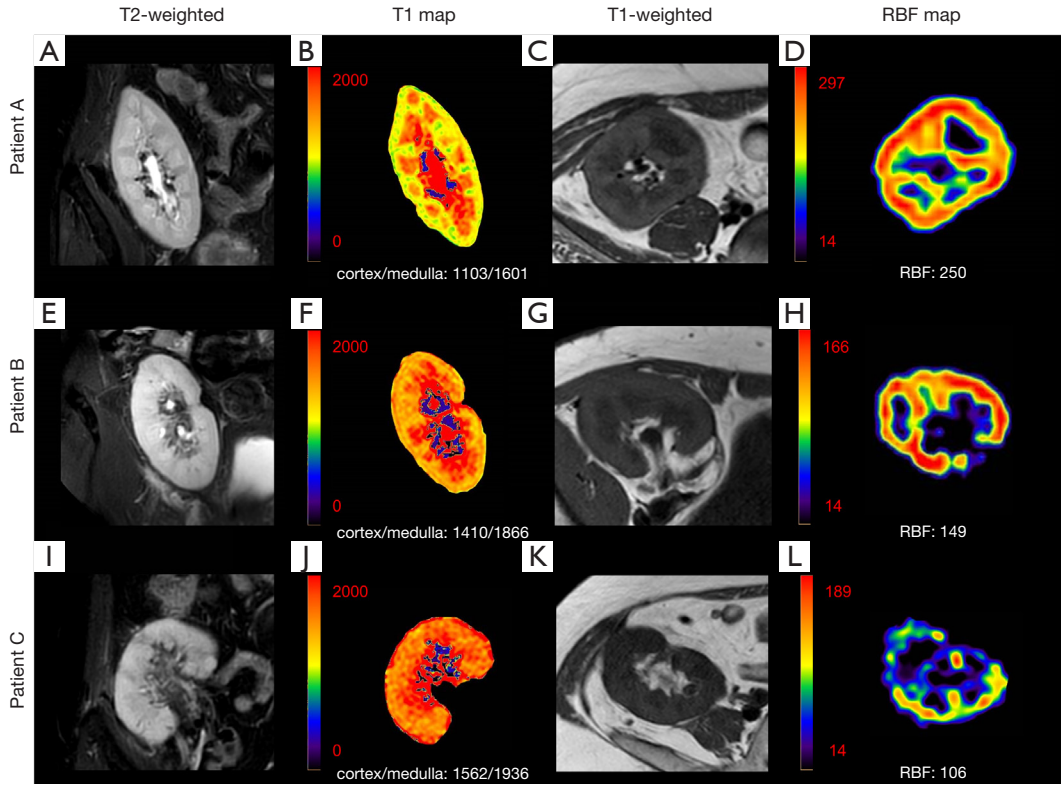

Figure 2 mpMRI in a 42-year-old woman (Patient A, from group A) with normal eGFR (eGFR, 109.1 mL/min/1.73 m^2), a 49-year-old man (Patient B, from group B) with moderately reduced eGFR (eGFR, 42.6 mL/min/1.73 m^2), and a 63-year-old woman (Patient C, from group C) with severely reduced eGFR (eGFR, 26.9 mL/min/1.73 m^2). Representative T2-weighted images (A,E,I), T1 maps (B,F,J), T1-weighted images (C,G,K), and RBF maps (D,H,L). The range of quantitative MRI parametric maps is displayed in the Figure, and the value of RBF and T1 are displayed at the bottom of the maps. Group A, patients with nor mal to mil dly reduced eGFR (e GFR ≥6 0 mL/min /1.73 m^2); G roup B, patients with moderately reduced eGFR (30≤ eGFR <60 mL/min/1.73 m^2); Group C, patients with severely reduced eGFR (eGFR <30 mL/min/1.73 m^2). mpMRI, multi-parametric magnetic resonance imaging; eGFR, estimated glomerular filtration rate; T1, longitudinal relaxation time; RBF, renal blood flow.

(r=0.569 and 0.672, respectively; P<0.001). Cortical T1 was negatively correlated with eGFR (r=–0.573, P<0.001). No significant correlation was found between medullary T1 and eGFR (P=0.68) (*Figure 3*).

Cortical T1 showed a positive correlation with the i and t scores (r=0.459 and 0.520, respectively; P=0.04 and 0.02, respectively). The ΔT1 was negatively correlated with the ci and ct scores (r=–0.502 and –0.452, respectively; P=0.02 and 0.04, respectively). The RBF showed a negative correlation with the ptc scores (r=–0.485, P=0.03). No significant correlations were found between the MRI parameters and the other Banff scores (all P>0.05) (*Figure 3*).

Diagnostic performances of ASL and T1 mapping

The areas under the curve (AUCs) of the ASL parameters (RBF), T1 mapping parameters (cortical T1 + ΔT1), and multi-parameter (RBF + cortical T1 + ΔT1) to discriminate between groups A and B were 0.740, 0.873, and 0.892, respectively. The diagnostic performance of the multi-parameter MRI was significantly better than that of ASL (P=0.03). While comparing groups B and C, RBF showed excellent diagnostic performance with an AUC of 0.729 [95% confidence interval (CI): 0.546–0.868]. When using 88 mL/100 g/min as the cut-off value for eGFR,

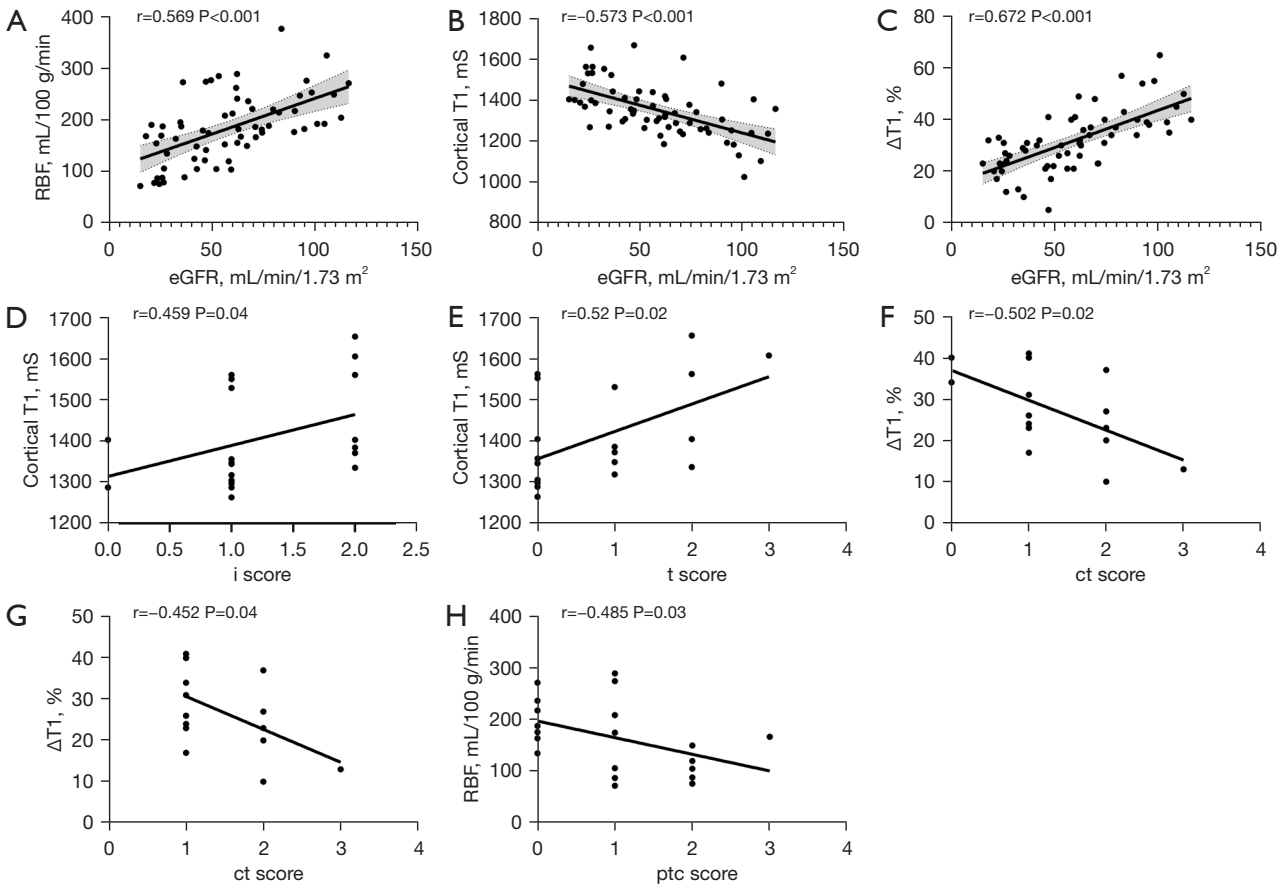

Figure 3 Correlation of MRI parameters with eGFR and Banff pathological scores of the renal allograft. Correlation of MRI parameters with eGFR (A-C). Correlation of MRI parameters with i, t, ci, ct, and ptc scores [in patients (n=20) who underwent biopsies] (D-H). The RBF and ΔT1 show a moderately positive correlation with eGFR (P<0.001 for both). Cortical T1 shows a moderately negative correlation with eGFR (P<0.001). Cortical T1 shows a moderately positive correlation with the i and t scores (P=0.04 and 0.02, respectively). The ΔT1 shows a moderately negative correlation with the ci and ct scores (P=0.02 and 0.05, respectively). The RBF shows a moderately negative correlation with ptc scores (P=0.03). MRI, magnetic resonance imaging; eGFR, estimated glomerular filtration rate; T1, longitudinal relaxation time; RBF, renal blood flow.

Table 2 Diagnostic efficiency of MRI parameters for distinguishing allografts with different renal functions

Parameters	Group A *vs.* Group B		Group B *vs.* Group C		Group A *vs.* Group C	
	AUC (95% CI)	P	AUC (95% CI)	P	AUC (95% CI)	P
ASL	0.740 (0.597–0.854)	0.004	0.729 (0.546–0.868)	0.02	0.923 (0.800–0.982)	<0.001
T1 mapping	0.873 (0.749–0.950)	<0.001	–	–	0.926 (0.803–0.983)	<0.001
mpMRI	0.892 (0.771–0.962)	<0.001	–	–	0.956 (0.846–0.995)	<0.001

The AUC, 95% CI, and P value is given. MRI, magnetic resonance imaging; AUC, area under the curve; CI, confidence interval; ASL, arterial spin labeling; ΔT1, 100% × (cortical T1 – medullary T1)/cortical T1; mpMRI, multi-parametric MRI (ASL + T1 mapping). Group A, patients with normal to mildly reduced eGFR (eGFR ≥60 mL/min/1.73 m^2); Group B, patients with moderately reduced eGFR (30≤ eGFR <60 mL/min/1.73 m^2); Group C, patients with severely reduced eGFR (eGFR <30 mL/min/1.73 m^2).

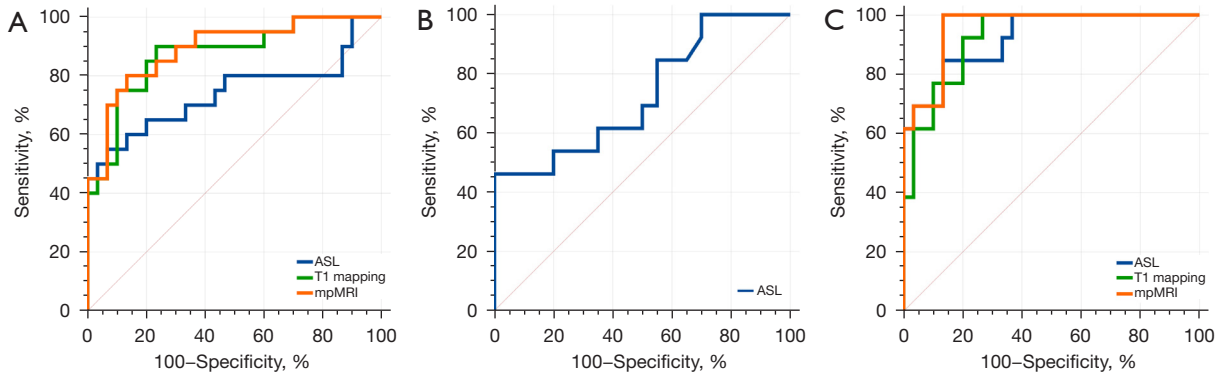

Figure 4 MRI quantitative parameters and multiple parameters (ASL combined with T1 mapping) distinguished allografts with different kidney functions. The AUC of ASL for distinguishing (A) Group A *vs.* Group B, (B) Group B *vs.* Group C, and (C) Group A *vs.* Group C are 0.740, 0.729, and 0.923, respectively. The AUC of T1 mapping for distinguishing (A) Group A *vs.* Group B, and (C) Group A *vs.* Group C are 0.873 and 0.926, respectively. The AUC of the multi-parameter for distinguishing (A) Group A *vs.* Group B, and (C) Group A *vs.* Group C is 0.892 and 0.956, respectively. Group A, patients with normal to mildly reduced eGFR (eGFR ≥60 mL/min/1.73 m^2); Group B, patients with m oderately reduced eGFR (30≤ eGFR <60 mL/min/1.73 m^2); Group C, patients with severely reduced eGFR (eGFR <30 mL/min/1.73 m^2). ASL, arterial spin labeling; mpMRI, multi-parametric MRI; MRI, magnetic resonance imaging; AUC, area under the curve.

the sensitivity was 46.2% and the specificity was 100.0%. The AUCs of the ASL parameters (RBF), T1 mapping parameters (cortical T1, ΔT1), and multi-parameter (RBF + cortical T1 + ΔT1) for identifying groups A and C were 0.923, 0.926, and 0.956, respectively (*Table 2*, *Figure 4*).

Discussion

Renal allograft injury is usually accompanied by changes in renal blood perfusion and microstructure, which can be detected using ASL and T1 mapping. In this study, the RBF, cortical T1, and ΔT1 of transplanted kidneys were moderately correlated with eGFR, suggesting that these parameters can reflect kidney function to a certain extent. This strongly indicated the feasibility of the combined assessment of kidney function using ASL and T1 mapping. In addition, moderate correlations were observed between the MRI parameters and Banff pathology scores for the diagnosis of renal allograft rejection and chronicity, suggesting that ASL and T1 mapping can provide important information for the clinical management of renal allografts.

In patients with long-term renal transplant survival, RBF was positively correlated with eGFR. The ASL allowed for clear differentiation between the stages of impaired kidney function. The number of capillaries and tubules decreases with impaired kidney function, leading to reduced renal perfusion, which can be detected noninvasively using ASL (25). Animal study has shown that ASL detects changes in renal perfusion corresponding to the degree of ischemia induction and correlates significantly with histological injury and kidney function (26). Wang *et al.* showed that renal cortical perfusion was positively correlated with peritubular capillary density measured using ASL (r=0.77; P<0.001), which confirmed the reliability of ASL in detecting renal perfusion (27).

Prolonged cortical T1 in the group with moderately to severely reduced eGFR may be due to the accumulation of water in the interstitia of transplanted kidney, which can be caused by pathophysiological changes, such as interstitial fibrosis, edema, and inflammation (28). In addition, high renal oxygen levels may lead to a decrease in T1 values (29,30). Interstitial fibrosis may lead to a decrease in peritubular capillaries causing hypoxia in the kidney, which may be another reason for prolonged cortical T1 values in renal allografts with impaired function. Peperhove *et al.* studied the T1 values in 49 kidney transplant patients, 52 lung transplant patients, and 14 healthy volunteers and observed a significant correlation between cortical T1 values, corticomedullary difference, and transplanted kidney function (31). The three groups did not show significant differences in medullary T1 values, which is consistent with the study by Bane *et al.* (32). One possible reason is that the water content in the renal tubule decreases due to renal injury, but increases due to inflammation and

edema, resulting in insignificant changes in the medullary T1 value (31). In our study, T1 values (cortical/medullary: 1,352±128/1,768±113 ms) were shorter than in those of patients, reported by Adams *et al.*, who underwent kidney transplantation >3 months before the examination (cortical/medullary: 1,615±47/2,004±68 ms) (33). The main reason for this difference was that they used a 3.0 T MRI in contrast to the 1.5 T MRI used by us. As B0 increases, T1 is usually lengthened (34).

Renal allograft rejection is one of the greatest issues for long-term allograft survival. Our study found a moderate correlation between MRI parameters and Banff histological scores in the diagnosis of renal allograft rejection. Cortical T1 was negatively correlated with both the i and t scores, and RBF was negatively correlated with the ptc scores. According to the 2012 Clinical Practice Guideline for the Care of Kidney Transplant Recipients (NKF-KDIGO), a biopsy should be performed when acute rejection of a transplanted kidney is highly suspected, and the anti-rejection treatment regimen should be adjusted according to the biopsy results (35,36). The Banff score directly impacts the clinical management of patients with transplanted kidneys. Therefore, multi-parametric MRI associated with Banff pathology scores can provide, to a certain extent, critical information for the clinical management of transplanted kidneys. There are few studies regarding the correlation between MRI findings and renal allograft rejection pathologies. Li *et al.* investigated the correlation between MRI and renal allograft rejection pathology in pediatric patients with kidney transplants and found that fractional anisotropy (FA) from diffusion tensor imaging (DTI) was negatively correlated with the i, t, and ptc scores (37).

Interstitial fibrosis and tubular atrophy are often accompanied by reduced kidney function and are unavoidable after kidney transplantation. In our study, ΔT1 was negatively correlated with the ci and ct scores, suggesting that the T1 mapping technique is sensitive and can be used to quantitatively assess changes in collagen deposition, tissue edema, and inflammation caused by interstitial fibrosis. Similarly, Friedli *et al.*, who performed T1 mapping in patients and mice with transplanted kidneys, found a negative correlation between the corticomedullary difference of T1 and interstitial fibrosis, which can be used for the assessment of transplanted kidney fibrosis (38). We found no significant correlations between interstitial fibrosis and RBF, which was different from the results of previous study regarding ASL (39). We noticed that most of the participants who underwent biopsies showed mild to moderate fibrosis of the allografts, which might have a slight influence on renal perfusion. In addition, non-fibrotic factors, such as renal arteriosclerosis, caused by poorly controlled hypertension and hyperlipidemia may also affect renal perfusion.

The combined application of ASL and T1 mapping facilitates a detailed noninvasive assessment of renal graft function, perfusion, and tissue microstructure, and allows for longitudinal long-term follow-up. A functional MRI is not an ideal substitute for biopsy, because it is not highly specific to the type of transplanted kidney pathology. However, the functional MRI can help detect subclinical and slowly progressive pathological changes that are often difficult to detect using biochemical markers or ultrasonography. Hence, it can provide key information for early intervention in the clinical management of transplanted kidneys.

This study had several limitations. First, we did not investigate the relationship between the MRI parameters and the pathological scores of each patient, and only a subset of patients who underwent biopsy were selected for the study. Therefore, a larger sample size should be considered in future studies. Second, we did not perform a long-term follow-up to analyze the detailed prognostic value of multi-parametric MRI. Third, the underlying pathological conditions causing renal impairment were inconsistent; hence, the MRI's differential diagnostic value for different diseases could not be determined.

In conclusion, the combined application of ASL and T1 mapping techniques can accurately assess the kidney function in patients with long-term renal transplant survival, and significant correlations were found between MRI parameters and Banff pathological scores. Therefore, it can serve as a new imaging biomarker for the comprehensive assessment of function and histological changes of transplanted kidneys and can provide reliable information for the clinical management of long-term surviving transplanted kidneys.

Acknowledgments

Funding: This work was supported by the Application Fundamental Research Program of the Jiangsu Provincial Health Commission's Elderly Health Project (Grant No. LK2021017), and Undergraduate Training Program for Innovation and Entrepreneurship Soochow University (No. 202310285070Z).

Footnote

Reporting Checklist: The authors have completed the STROBE reporting checklist. Available at https://qims.amegroups.com/article/view/10.21037/qims-23-1577/rc

Conflicts of Interest: All authors have completed the ICMJE uniform disclosure form (available at https://qims.amegroups.com/article/view/10.21037/qims-23-1577/coif). P.W. is an employee of Philips Healthcare. The other authors have no conflicts of interest to declare.

Ethical Statement: The authors are accountable for all aspects of the work in ensuring that questions related to the accuracy or integrity of any part of the work are appropriately investigated and resolved. The study was conducted in accordance with the Declaration of Helsinki (as revised in 2013). The study was approved by ethics board of the First Affiliated Hospital of Soochow University and informed consent was obtained from all the patients.

References

1. Nankivell BJ, Alexander SI. Rejection of the kidney allograft. N Engl J Med 2010;363:1451-62.
2. Elbadri A, Traynor C, Veitch JT, O'Kelly P, Magee C, Denton M, O'Sheaghdha C, Conlon PJ. Factors affecting eGFR 5-year post-deceased donor renal transplant: analysis and predictive model. Ren Fail 2015;37:417-23.
3. Abecassis M, Bartlett ST, Collins AJ, Davis CL, Delmonico FL, Friedewald JJ, Hays R, Howard A, Jones E, Leichtman AB, Merion RM, Metzger RA, Pradel F, Schweitzer EJ, Velez RL, Gaston RS. Kidney transplantation as primary therapy for end-stage renal disease: a National Kidney Foundation/Kidney Disease Outcomes Quality Initiative (NKF/KDOQITM) conference. Clin J Am Soc Nephrol 2008;3:471-80.
4. Earley A, Miskulin D, Lamb EJ, Levey AS, Uhlig K. Estimating equations for glomerular filtration rate in the era of creatinine standardization: a systematic review. Ann Intern Med 2012;156:785-95.
5. Myers GL, Miller WG, Coresh J, Fleming J, Greenberg N, Greene T, Hostetter T, Levey AS, Panteghini M, Welch M, Eckfeldt JH; . Recommendations for improving serum creatinine measurement: a report from the Laboratory Working Group of the National Kidney Disease Education Program. Clin Chem 2006;52:5-18.
6. Coca SG, Yalavarthy R, Concato J, Parikh CR. Biomarkers for the diagnosis and risk stratification of acute kidney injury: a systematic review. Kidney Int 2008;73:1008-16.
7. Solez K, Racusen LC. The Banff classification revisited. Kidney Int 2013;83:201-6.
8. American Society of Nephrology Renal Research Report. J Am Soc Nephrol 2005;16:1886-903.
9. Schwarz A, Gwinner W, Hiss M, Radermacher J, Mengel M, Haller H. Safety and adequacy of renal transplant protocol biopsies. Am J Transplant 2005;5:1992-6.
10. Moledina DG, Luciano RL, Kukova L, Chan L, Saha A, Nadkarni G, Alfano S, Wilson FP, Perazella MA, Parikh CR. Kidney Biopsy-Related Complications in Hospitalized Patients with Acute Kidney Disease. Clin J Am Soc Nephrol 2018;13:1633-40.
11. Chandarana H, Lee VS. Renal functional MRI: Are we ready for clinical application? AJR Am J Roentgenol 2009;192:1550-7.
12. Thoeny HC, De Keyzer F. Diffusion-weighted MR imaging of native and transplanted kidneys. Radiology 2011;259:25-38.
13. Eisenberger U, Thoeny HC, Binser T, Gugger M, Frey FJ, Boesch C, Vermathen P. Evaluation of renal allograft function early after transplantation with diffusion-weighted MR imaging. Eur Radiol 2010;20:1374-83.
14. Kirpalani A, Hashim E, Leung G, Kim JK, Krizova A, Jothy S, Deeb M, Jiang NN, Glick L, Mnatzakanian G, Yuen DA. Magnetic Resonance Elastography to Assess Fibrosis in Kidney Allografts. Clin J Am Soc Nephrol 2017;12:1671-9.
15. Artz NS, Wentland AL, Sadowski EA, Djamali A, Grist TM, Seo S, Fain SB. Comparing kidney perfusion using noncontrast arterial spin labeling MRI and microsphere methods in an interventional swine model. Invest Radiol 2011;46:124-31.
16. Cutajar M, Thomas DL, Hales PW, Banks T, Clark CA, Gordon I. Comparison of ASL and DCE MRI for the non-invasive measurement of renal blood flow: quantification and reproducibility. Eur Radiol 2014;24:1300-8.

17. Radenkovic D, Weingärtner S, Ricketts L, Moon JC, Captur G. T(1) mapping in cardiac MRI. Heart Fail Rev 2017;22:415-30.
18. Li Z, Sun J, Hu X, Huang N, Han G, Chen L, Zhou Y, Bai W, Yang X. Assessment of liver fibrosis by variable flip angle T1 mapping at 3.0T. J Magn Reson Imaging 2016;43:698-703.
19. Poindron V, Chatelus E, Canuet M, Gottenberg JE, Arnaud L, Gangi A, Gavand PE, Guffroy A, Korganow AS, Germain P, Sibilia J, El Ghannudi S, Martin T. T1 mapping cardiac magnetic resonance imaging frequently detects subclinical diffuse myocardial fibrosis in systemic sclerosis patients. Semin Arthritis Rheum 2020;50:128-34.
20. Warnica W, Al-Arnawoot A, Stanimirovic A, Thavendiranathan P, Wald RM, Pakkal M, Karur GR, Wintersperger BJ, Rac V, Hanneman K. Clinical Impact of Cardiac MRI T1 and T2 Parametric Mapping in Patients with Suspected Cardiomyopathy. Radiology 2022;305:319-26.
21. Levey AS, Stevens LA, Schmid CH, Zhang YL, Castro AF 3rd, Feldman HI, Kusek JW, Eggers P, Van Lente F, Greene T, Coresh J; CKD-EPI (Chronic Kidney Disease Epidemiology Collaboration). A new equation to estimate glomerular filtration rate. Ann Intern Med 2009;150:604-12.
22. Sis B, Mengel M, Haas M, Colvin RB, Halloran PF, Racusen LC, et al. Banff '09 meeting report: antibody mediated graft deterioration and implementation of Banff working groups. Am J Transplant 2010;10:464-71.
23. Solez K, Colvin RB, Racusen LC, Haas M, Sis B, Mengel M, et al. Banff 07 classification of renal allograft pathology: updates and future directions. Am J Transplant 2008;8:753-60.
24. Williams WW, Taheri D, Tolkoff-Rubin N, Colvin RB. Clinical role of the renal transplant biopsy. Nat Rev Nephrol 2012;8:110-21.
25. Cai XR, Yu J, Zhou QC, Du B, Feng YZ, Liu XL. Use of intravoxel incoherent motion MRI to assess renal fibrosis in a rat model of unilateral ureteral obstruction. J Magn Reson Imaging 2016;44:698-706.
26. Hueper K, Gutberlet M, Rong S, Hartung D, Mengel M, Lu X, Haller H, Wacker F, Meier M, Gueler F. Acute kidney injury: arterial spin labeling to monitor renal perfusion impairment in mice-comparison with histopathologic results and renal function. Radiology 2014;270:117-24.
27. Wang W, Yu Y, Wen J, Zhang M, Chen J, Cheng D, Zhang L, Liu Z. Combination of Functional Magnetic Resonance Imaging and Histopathologic Analysis to Evaluate Interstitial Fibrosis in Kidney Allografts. Clin J Am Soc Nephrol 2019;14:1372-80.
28. Schmidbauer M, Rong S, Gutberlet M, Chen R, Bräsen JH, Hartung D, Meier M, Wacker F, Haller H, Gueler F, Greite R, Derlin K. Diffusion-Weighted Imaging and Mapping of T1 and T2 Relaxation Time for Evaluation of Chronic Renal Allograft Rejection in a Translational Mouse Model. J Clin Med 2021;10:4318.
29. O'Connor JP, Jackson A, Buonaccorsi GA, Buckley DL, Roberts C, Watson Y, Cheung S, McGrath DM, Naish JH, Rose CJ, Dark PM, Jayson GC, Parker GJ. Organ-specific effects of oxygen and carbogen gas inhalation on tissue longitudinal relaxation times. Magn Reson Med 2007;58:490-6.
30. Jones RA, Ries M, Moonen CT, Grenier N. Imaging the changes in renal T1 induced by the inhalation of pure oxygen: a feasibility study. Magn Reson Med 2002;47:728-35.
31. Peperhove M, Vo Chieu VD, Jang MS, Gutberlet M, Hartung D, Tewes S, Warnecke G, Fegbeutel C, Haverich A, Gwinner W, Lehner F, Bräsen JH, Haller H, Wacker F, Gueler F, Hueper K. Assessment of acute kidney injury with T1 mapping MRI following solid organ transplantation. Eur Radiol 2018;28:44-50.
32. Bane O, Hectors SJ, Gordic S, Kennedy P, Wagner M, Weiss A, Khaim R, Yi Z, Zhang W, Delaney V, Salem F, He C, Menon MC, Lewis S, Taouli B. Multiparametric magnetic resonance imaging shows promising results to assess renal transplant dysfunction with fibrosis. Kidney Int 2020;97:414-20.
33. Adams LC, Bressem KK, Scheibl S, Nunninger M, Gentsch A, Fahlenkamp UL, Eckardt KU, Hamm B, Makowski MR. Multiparametric Assessment of Changes in Renal Tissue after Kidney Transplantation with Quantitative MR Relaxometry and Diffusion-Tensor Imaging at 3 T. J Clin Med 2020;9:1551.
34. Wolf M, de Boer A, Sharma K, Boor P, Leiner T, Sunder-Plassmann G, Moser E, Caroli A, Jerome NP. Magnetic resonance imaging T1- and T2-mapping to assess renal structure and function: a systematic review and statement paper. Nephrol Dial Transplant 2018;33:ii41-50.
35. Chadban SJ, Ahn C, Axelrod DA, Foster BJ, Kasiske BL, Kher V, Kumar D, Oberbauer R, Pascual J, Pilmore HL, Rodrigue JR, Segev DL, Sheerin NS, Tinckam KJ, Wong G, Balk EM, Gordon CE, Earley A, Rofeberg V, Knoll GA. Summary of the Kidney Disease: Improving Global Outcomes (KDIGO) Clinical Practice Guideline on the

Evaluation and Management of Candidates for Kidney Transplantation. Transplantation 2020;104:708-14.
36. Creeley C, Dikranian K, Dissen G, Martin L, Olney J, Brambrink A. Propofol-induced apoptosis of neurones and oligodendrocytes in fetal and neonatal rhesus macaque brain. Br J Anaesth 2013;110 Suppl 1:i29-38.
37. Li Y, Lee MM, Worters PW, MacKenzie JD, Laszik Z, Courtier JL. Pilot Study of Renal Diffusion Tensor Imaging as a Correlate to Histopathology in Pediatric Renal Allografts. AJR Am J Roentgenol 2017;208:1358-64.
38. Friedli I, Crowe LA, Berchtold L, Moll S, Hadaya K, de Perrot T, Vesin C, Martin PY, de Seigneux S, Vallée JP. New Magnetic Resonance Imaging Index for Renal Fibrosis Assessment: A Comparison between Diffusion-Weighted Imaging and T1 Mapping with Histological Validation. Sci Rep 2016;6:30088.
39. Yu YM, Wang W, Wen J, Zhang Y, Lu GM, Zhang LJ. Detection of renal allograft fibrosis with MRI: arterial spin labeling outperforms reduced field-of-view IVIM. Eur Radiol 2021;31:6696-707.

Cite this article as: Jiang B, Li J, Wan J, Tian Y, Wu P, Xu R, Yu Y, Wang X, Hu L, Zhu M. Arterial spin labeling combined with T1 mapping for assessment of kidney function and histopathology in patients with long-term renal transplant survival after kidney transplantation. Quant Imaging Med Surg 2024;14(3):2415-2425. doi: 10.21037/qims-23-1577

Supplementary

Table S1 Indication for renal biopsy, biopsy result, and Banff scores for patients who underwent biopsy

	Indication for renal biopsy	Biopsy results	Banff scores					
			i	t	g	ptc	ci	ct
1	Surveillance biopsy	IgA nephropathy	1	0	3	0	0	1
2	Elevated serum creatinine value	1. segmental glomerulosclerosis, arteriolar hyalinization 2. IgA nephropathy	1	0	0	0	2	2
3	Albuminuria	IgA nephropathy	0	0	0	0	1	1
4	Elevated serum creatinine value	1. borderline change; 2. membranous nephropathy	1	1	0	1	1	1
5	Elevated serum creatinine value	1. acute T-cell-mediated rejection; 2. chronic antibody-mediated rejection	2	2	0	2	0	1
6	Albuminuria	1. focal segmental glomerulosclerosis; 2. mild chronic tubulointerstitial injury, arteriolar hyalinization	1	0	0	0	1	1
7	Elevated serum creatinine value; albuminuria	1. acute T-cell-mediated rejection; 2. antibody-mediated rejection	2	3	0	3	1	1
8	Elevated serum creatinine value	1. antibody-mediated rejection; 2. partial glomerulosclerosis, mild chronic tubulointerstitial injury	1	0	0	2	1	1
9	Surveillance biopsy	1. focal segmental glomerulosclerosis; 2. acute T-cell-mediated rejection	1	0	1	2	1	1
10	Recurrent diarrhea with fever	partial and segmental glomerulosclerosis, moderate chronic tubulointerstitial injury, arteriolar hyalinization	1	0	0	0	2	2
11	Elevated serum creatinine value	1. acute T-cell-mediated rejection; 2. partial glomerulosclerosis with mild chronic tubulointerstitial injury, arteriolar hyalinization	2	2	0	1	1	1
12	Follow-up biopsy to evaluate for rejection	1. chronic antibody-mediated rejection; 2. mild chronic tubulointerstitial injury with partial glomerulosclerosis	2	1	0	1	2	2
13	Elevated serum creatinine value	antibody-mediated rejection	1	1	0	1	1	1
14	Elevated serum creatinine value	1. IgA nephropathy; 2. segmental glomerulosclerosis, severe chronic tubulointerstitial injury	1	0	0	0	3	3
15	Elevated serum creatinine value	1. acute T-cell-mediated rejection; 2. partial glomerulosclerosis with mild chronic tubulointerstitial injury	2	2	0	1	1	1
16	Elevated serum creatinine value	1. chronic antibody-mediated rejection; 2. IgA nephropathy; 3. segmental glomerulosclerosis, moderate chronic tubulointerstitial injury	0	0	2	1	2	2
17	Elevated serum creatinine value	BK virus nephropathy	2	1	0	0	1	1
18	Elevated serum creatinine value	1. chronic antibody-mediated rejection; 2. acute T-cell-mediated rejection	2	2	2	2	1	1
19	Elevated serum creatinine value	1. thrombotic microangiopathy; 2. moderate chronic tubulointerstitial injury with glomerulosclerosis	1	1	3	2	2	2
20	Elevated serum creatinine value	1. acute tubular necrosis; 2. antibody-mediated rejection; 3.focal segmental glomerulosclerosis; 4. mild chronic tubulointerstitial injury, arteriolar hyalinization	1	0	0	1	1	1

https://dx.doi.org/10.21037/qims-23-1577